AUTOMATED QUANTIFICATION OF WHITE MATTER HYPERINTENSITY BURDEN USING MPRAGE AND FLAIR IMAGES FROM A LARGE POPULATION

by

KEITH MCLEOD HULSEY

Presented to the Faculty of the Graduate School of
The University of Texas at Arlington in Partial Fulfillment
of the Requirements
for the Degree of

MASTER OF SCIENCE IN BIOMEDICAL ENGINEERING

THE UNIVERSITY OF TEXAS AT ARLINGTON

December 2008

To all who need a new beginning.

ACKNOWLEDGEMENTS

The opportunity to pursue this degree came at an important time in my life. I had arrived at a place where I lacked clear direction and needed a worthy passion. Entering the field of medical imaging returned me to my dreams of twenty years ago.

I feel a deep appreciation to the many people who have encouraged me. Dr. Hanli Liu introduced me to the modalities of medical imaging and encouraged me in my projects. Dr. Kaundinya Gopinath directed me to important background reading and helped feed my curiosity. Dr. Vikram Kodibagkar fielded my physics questions when I was not even sure how to pose them. Dr. Matthew Lewis introduced me to magical properties of cutting-edge image processing techniques. I owe a debt of gratitude to Dr. Roddy McColl. His direction, encouragement and support have been vital to this project and to my academic pursuit.

Several others have contributed in concrete ways to my work. Dr. Ron Peshock provided access to data and the hardware required for image processing. Dr. Kevin King evaluated the images making my algorithm refinement less subjective. Dr. Myron Weiner provided data quantifying the cognitive function of the study subjects. Colby Ayers provided invaluable support for the statistical analysis.

My wife's patience and support have allowed me the opportunity to direct my attention to new goals and dreams. I love you Nancy. Thanks for sharing the journey with me.

For the breath of life and the hope of glory I am forever grateful to my God in Jesus Christ.

November 20, 2008

ABSTRACT

White Matter Hyperintensity burden, as observed in T2 and proton weighted MR images, is associated with several health factors such as decreased cognitive ability, hypertension, diabetes and cerebrovascular disease. An algorithm was developed to automatically estimate WMH burden from pairs of MPRAGE and FLAIR images which is robust and requires essentially no operator involvement. The WMH burden estimation generated by this fully automated algorithm has been shown to correlate well with known risk factors for WMH burden.

TABLE OF CONTENTS

LIST OF FIGURES

LIST OF TABLES

CHAPTER 1

INTRODUCTION

The study of brain aging and brain health has been greatly facilitated by the advent of non-invasive brain imaging. Many brain lesions which are easily identified in certain modalities of imaging would otherwise remain undetected. White matter hyperintensities(WMH) are lesions of the white matter which appear bright in T2 and proton weighted MR images. WMH burden has been associated with several health factors such as decreased cognitive ability, hypertension, diabetes and cerebrovascular disease.[1] Available methods of using MR images from 3T scanners to assess WMH burden require some degree of operator involvement.[2] As a result, assessing WMH burden in large population studies requires significant allocation of resources. An algorithm was developed in this study for automatically estimating WMH burden from pairs of MPRAGE and FLAIR images. The algorithm was developed to operate independently of operator interaction.

This study utilized pairs of FLAIR and MPRAGE images for over 1000 subjects. The MPRAGE images were segmented to locate the white matter and the FLAIR images were used to identify hyperintensities in the white matter. The algorithm was refined through comparisons of the WMH burden estimates with subjective ratings of a subset of the images. Once the algorithm refinement was completed, the algorithm was validated by comparing the WMH burden estimates with subjective ratings from a second subset of the images.

The sensitivity of the algorithm was evaluated by investigating whether correlations between WMH burden and several known risk factors could be detected.

The factors investigated were age, hypertension, reduced cognitive function, diabetes, gender and ethnicity. Potential interactions of the factors with age were taken into account when considering the other factors.

Seven hypotheses were laid out before the study was conducted.

1) The algorithm would be assumed to be valid if the agreement of the WMH burden estimates with the subjective ratings were significantly greater than chance, and the agreement between the WMH burden estimates and the subjective ratings were at least as good for a test data set as it was for the training data set at a P value less than 0.05.

2) The algorithm would be assumed to be sufficiently sensitive to detect the age factor if the slope from a regression of WMH burden estimate with age were positive at a P value less than 0.05.

3) The algorithm would be assumed to be sufficiently sensitive to detect the hypertension factor if the average WMH burden estimate for subjects with hypertension were greater than the average WMH burden estimate for subjects without hypertension after the WMH burden estimate had been corrected for age at a P value less than 0.05.

4) The algorithm would be assumed to be sufficiently sensitive to detect the reduced cognitive function factor if the slope of the MOCA factor from a regression of WMH burden estimate with age and MOCA score were negative at a P value less than 0.05.

5) The algorithm would be assumed to be sufficiently sensitive to detect the diabetes factor if the average WMH burden estimate for subjects with diabetes were greater than the average WMH burden estimate for subjects without diabetes after the WMH burden estimate had been corrected for age at a P value less than 0.05.

6) The algorithm would be assumed to be sufficiently sensitive to detect the gender factor if the average WMH burden estimate for female subjects were greater than the

average WMH burden estimate for male subjects after the WMH burden estimate had been corrected for age at a P value less than 0.05.

7) The algorithm would be assumed to be sufficiently sensitive to detect the ethnicity factor if the WMH burden estimates for the four ethnicity groupings were not from a single distribution after the WMH burden estimate had been corrected for age at a P value less than 0.05.

CHAPTER 2

METHODS

2.1 Introduction

A collection of images for 1006 subjects was obtained from the Dallas Heart Study for this study. Of this collection, a subset had been assessed for WMH burden and the subjective ratings were made available. A portion of the rated images was used for developing and refining an algorithm to automatically estimate WMH burden. The remaining rated images were used to assess the accuracy of the algorithm. The utility of the algorithm was further assess by evaluating correlations between the WMH burden estimate and certain biomarkers that were available for the subjects. It is beyond the scope of this study to draw conclusions about the WMH burden of participants in the Dallas Heart Study. The subjects whose data were used in the current study were not a representative sample of the population investigated in the Dallas Heart Study, making it inappropriate to draw conclusions regarding the WMH burden of the DHS population.

The images used in this study were MRI images of the heads of 1006 subjects acquired between 10/19/07 and 10/20/08 using MPRAGE and FLAIR pulse sequences on the Philips Medical Systems 3T MR scanner located at St. Paul Hospital, Dallas, Texas. The MPRAGE images were acquired with a TR of 9.7 ms, TE of 5.75 ms, and voxel size of 1mm x 0.9 mm x 0.9 mm. The FLAIR images were acquired with a TR of 11.0 sec, TE of 130 ms, TI of 2.80 sec, and voxel size of 5 mm x 0.45 mm x 0.45 mm. The patient data used in this study were obtained from the Reynolds database held at the University of Texas Southwestern Medical Center.

White matter hyperintensities are features which show up bright in T2 or proton weighted MR images, such as the FLAIR images used in this study which were strongly T2 weighted. In order to distinguish WMH from other bright structures in the FLAIR images, the search for WMH was restricted to white matter regions. Segmentation of the FLAIR images into white matter regions and gray matter regions based on intensity was not practical because the contrast between these regions in the FLAIR images was too small. The contrast between white matter and gray matter regions was significantly greater in the MPRAGE images because of strong T1 weighting. Therefore, the MPRAGE images were used for segmentation and the segmentation information was used to generate white matter and gray matter maps for the FLAIR images.

2.2 Image Processing Pipeline

The image processing conducted in this study employed freely available software and brain atlases. These were used to generate white matter masks for MPRAGE images, to register MPRAGE white matter masks to the corresponding FLAIR image, and to identify WMH through the application of a global threshold. A flow diagram of the image processing used in this study is presented in Figure 2.1.

The FSL library of programs[3] was used extensively for this project. The MR images had to be reformatted in preparation for image manipulation with FSL software. The images were retrieved from the Dallas Heart Study server where they were stored as collections of 2D DICOM format images. Software available in the AFNI library[4] was used to combine the 2D images into 3D NIFTI format images. Images of one of the subjects at points along the image processing chain are displayed in Figures 2.2 - 2.8. Figure 2.2 shows axial slices of the MPRAGE and FLAIR images after they were reformatted in preparation for processing with FSL software.

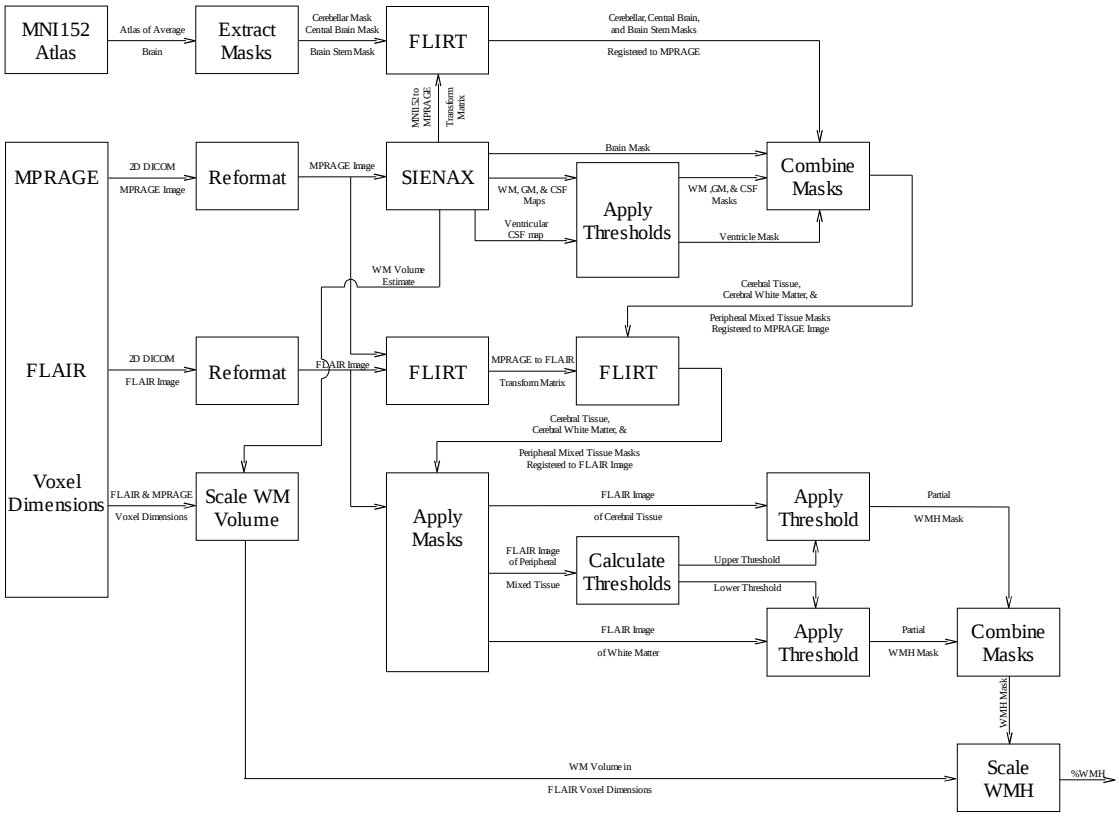

Figure 2.1. WMH Burden Estimation Flow Diagram.

The FSL routine SIENAX was used to remove the skull from the MPRAGE image and to segment the brain into the three classes of cerebrospinal fluid(CSF), white matter and gray matter. The data files retained from the SIENAX output were files containing a text SIENAX report, a brain mask, a separate probability map for each segmentation class, a probability map for ventricular CSF, and a matrix specifying the transformation required to register MNI152 atlases to the MPRAGE image.

Masks of the cerebellum and brain stem were created from the MNI152 atlas. These masks were then spatially transformed, using the transformation matrix produced by SIENAX, to correlate spatially with the cerebellum and brain stem of the MPRAGE image. The whole brain mask generated by SIENAX was then modified

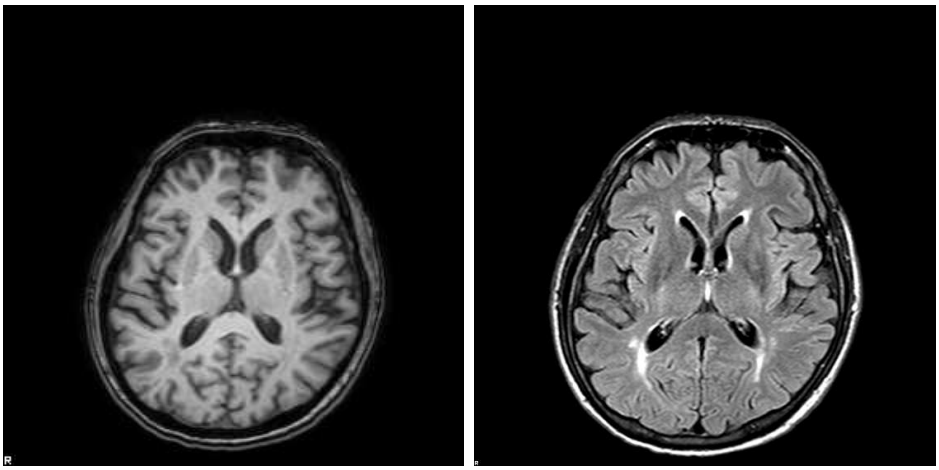

Figure 2.2. Representative MPRAGE and FLAIR Images. These images were acquired from the same subject. The image on the left was acquired with an MPRAGE sequence. The image on the right was acquired with a FLAIR sequence.

using these masks plus the ventricular CSF mask from SIENAX to generate a mask for the cerebrum in the MPRAGE image. Figure 2.3 shows an axial slice of the MPRAGE image with an overlay of the brain mask on the left and an overlay of the modified brain mask on the right.

A cerebral white matter mask was generated from the SIENAX white matter probability map. This was accomplished by applying a threshold of 0.5, meaning that only those voxels with at least a 50% chance of being white matter were included in the mask. Figure 2.4 shows the MPRAGE image overlaid with the white matter probability map on the left and the white matter mask on the right.

The probability map for CSF output by SIENAX was used to identify the voxels having at least a 10% chance of being CSF in the MPRAGE. These voxels were removed from cerebral brain mask generating a cerebral tissue mask for the MPRAGE image. A central brain mask was created from the MNI152 atlas and transformed so that it would be spatially registered to the MPRAGE image. The central brain mask was then used to exclude the central portion of the white matter

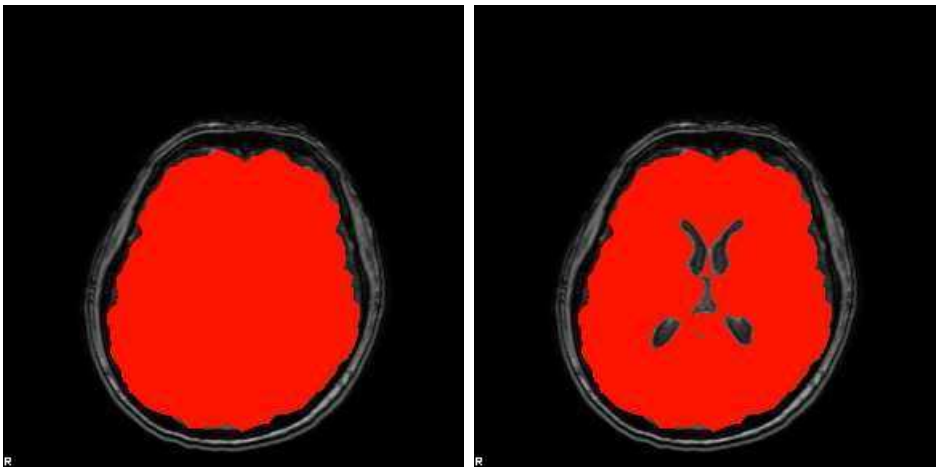

Figure 2.3. Brain Masks Overlaying an MPRAGE Image. The image on the left is overlaid with the brain mask from BET in red. The image on the right is overlaid with a brain mask which has the ventricles excluded from the mask.

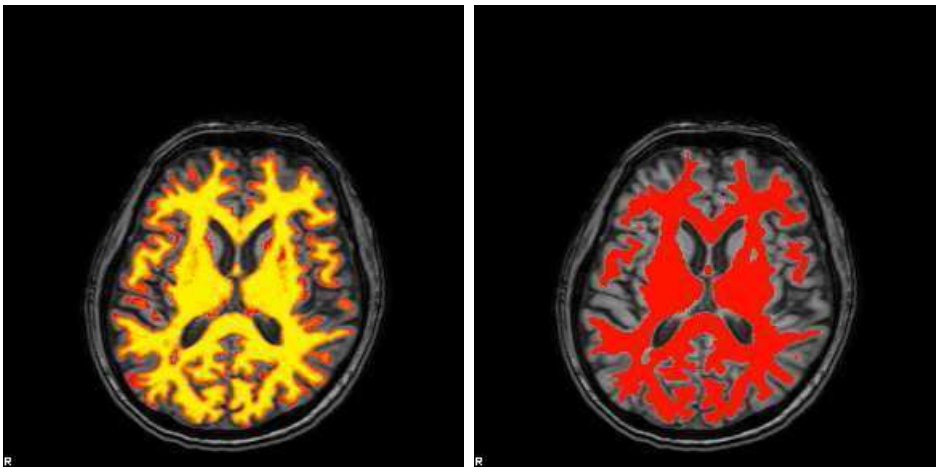

Figure 2.4. White Matter Masks Overlaying an MPRAGE Image. The image on the left is overlaid with a white matter probability map (yellow=high probability, red=low probability, gray scale=0 probability). The image on the right is overlaid with a binary white matter mask.

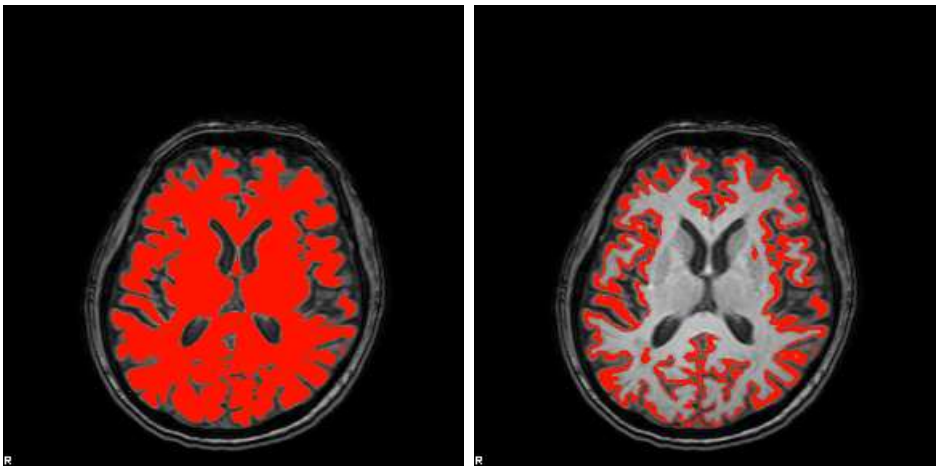

Figure 2.5. Other Tissue Masks Overlaying an MPRAGE Image. The image on the left is overlaid with a mask of cerebral tissue (white and gray matter). The image on the right is overlaid with a mask of peripheral mixed tissue.

probability map. A threshold was applied to the resulting map to produce a mask of peripheral mixed tissue voxels. Voxels with a probability of being white matter that was between 0% and 50% were included in the mask. Figure 2.5 shows the MPRAGE image overlaid with the cerebral tissue mask on the left and overlaid with the peripheral mixed tissue mask on the right.

The FSL routine FLIRT was used to generate a spatial transformation matrix to describe the transformation required to register the MPRAGE image for a subject to the subject's corresponding FLAIR image. Using the MPRAGE and FLAIR images as input, FLIRT calculated a transformation matrix with 12 degrees of freedom that maximized the cost function of normalized mutual information. Figure 2.6 shows the MPRAGE in its original spatial dimensions on the left and the MPRAGE after the spatial transformation on the right. There is little difference in the two visually because the orientation of the brain in the MPRAGE and the FLAIR images was nearly identical. The most important difference was that the MPRAGE image was resampled to have voxels that corresponded to the voxels in the FLAIR image.

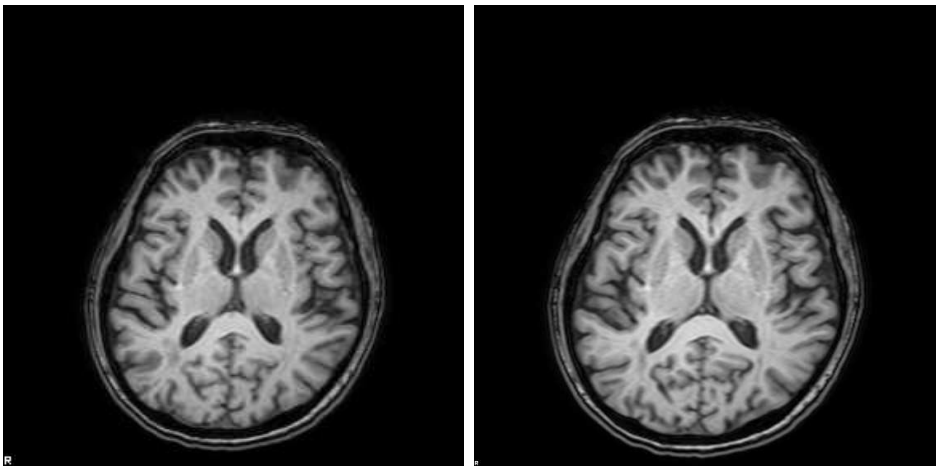

Figure 2.6. Spatially Transformed MPRAGE Image.
The image on the left is an MPRAGE image. The image on the right is the MPRAGE image spatial transformed to be registered to the FLAIR image.

The MPRAGE to FLAIR spatial transformation matrix was then applied with FLIRT to the cerebral tissue mask, the cerebral white matter mask, and the cerebral periphery mixed tissue mask. The three masks were applied to the FLAIR image resulting in a FLAIR image of cerebral tissue, a FLAIR image of cerebral white matter, and a FLAIR image of cerebral periphery mixed tissue. Figure 2.7 shows the FLAIR image overlaid with the cerebral white matter mask on the left and overlaid with the cerebral tissue mask on the right.

A histogram of the cerebral periphery mixed tissue image was used to generate threshold values to be applied to the images of the other tissue types. The histogram collection was restricted to the periphery of the image to exclude most of the hyperintensities. The mixed tissue was used to estimate mean and variance characteristics of the MR signal for a consistent sampling of brain tissue.

A threshold value 3.0 standard deviations above the mean of the cerebral periphery mixed tissue image was applied to the cerebral white matter FLAIR image. A mask was produced of the voxels with FLAIR intensities above the threshold. Since

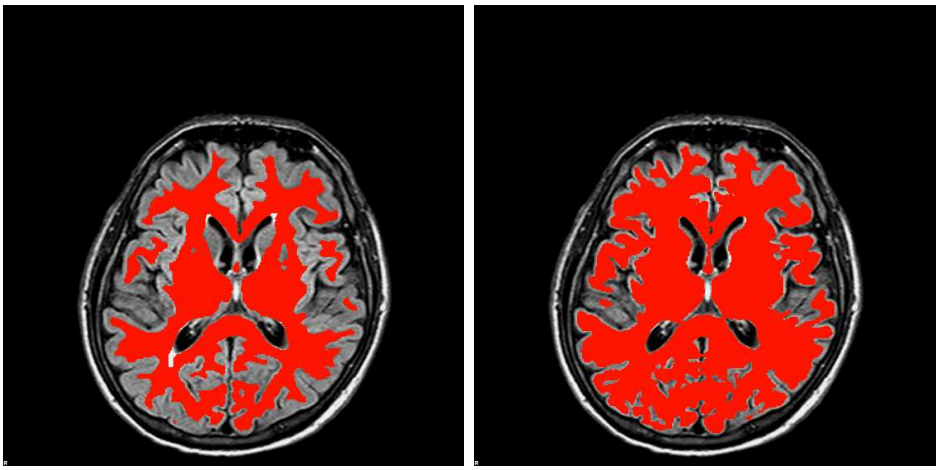

Figure 2.7. Tissue and WM Masks Overlaying a FLAIR Image. The image on the left is overlaid with the cerebral white matter mask. The image on the right is overlaid with the cerebral tissue mask.

the only voxels compared to the threshold were located in the white matter, higher intensity gray matter voxels were excluded. However, white matter voxels inappropriately classified by SIENAX as gray matter were also excluded. This issue was addressed by using a second threshold.

A second threshold value 3.5 standard deviations above the mean of the cerebral periphery mixed tissue image was also calculated. This threshold was applied to the cerebral tissue image. The resulting mask included hyperintense voxels in the white matter which had been misclassified as gray matter. The white matter voxels which were misclassified tended to be voxels with intensities larger than this second threshold. This higher threshold, however, excluded many of the brighter gray matter voxels that would have been included with the lower threshold. Figure 2.8 shows the FLAIR image overlaid with the WMH mask generated from the white matter on the upper left, overlaid with the WMH mask generated from the cerebral tissue on the upper right, and overlaid with the combined WMH mask on the lower right. The FLAIR image is shown without an overlay on the lower left for comparison.

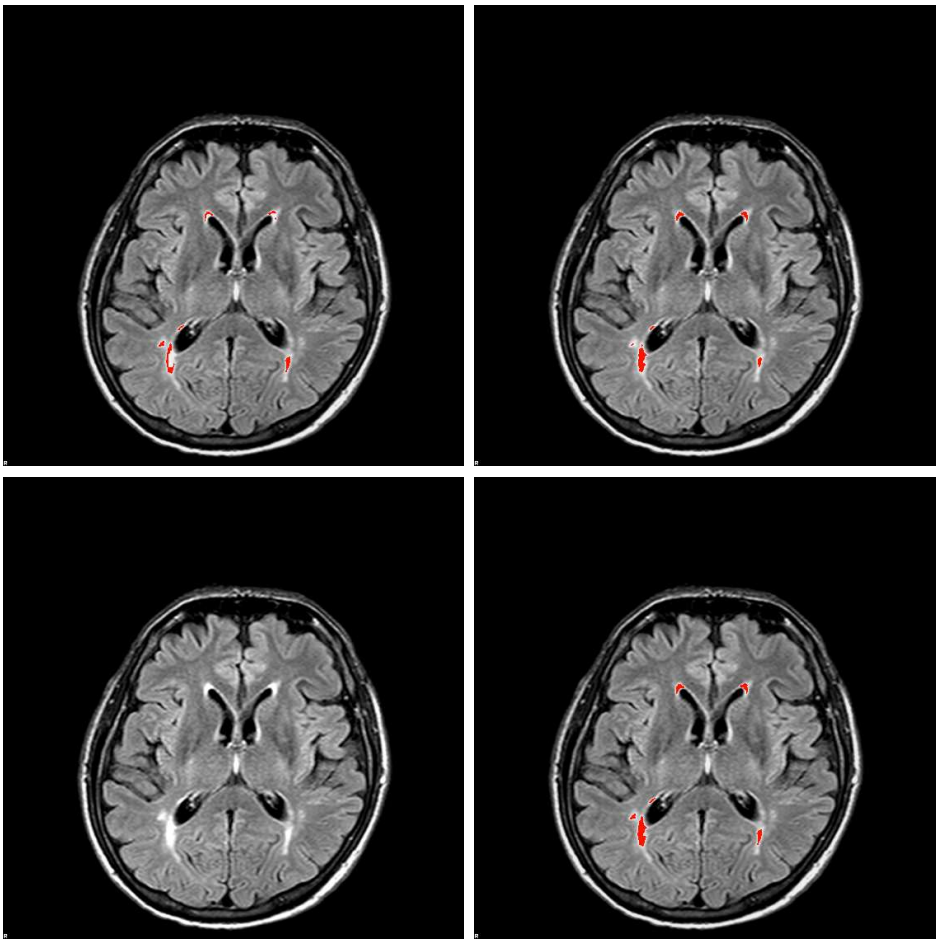

Figure 2.8. White Matter Hyperintensity Masks on FLAIR Image. On the upper left WMH from white matter is in red. On the upper right WMH from white and gray matter is in red. On the lower right WMH combined from both is in red.

The number of voxels of WMH was divided by the total white matter volume reported in the SIENAX report. This ratio was then scaled by the ratio of the MPRAGE voxel volume to the FLAIR voxel volume and reported as a percentage. The voxel volumes were calculated from voxel dimension data collected from DICOM headers for the images.

2.3 Variables for Refining the WMH Burden Estimation Algorithm

Two parameters were varied in setting the intensity threshold above which voxels were designated as hyperintense. In general, the mean and standard deviation of intensity was calculated for a portion of the image and the threshold was set to a value that was a specified number of standard deviations above the mean. The parameters specifying the number of standard deviations used to calculate the threshold and specifying which portion of the image was to be used for calculating the mean and standard deviation were varied.

Three basic methods were employed for delineating the portion of the image to use for calculating the threshold. The first was to select all areas of the FLAIR image which were identified as cerebral tissue in the MPRAGE image. The image intensities in these areas were used to calculate the threshold.

The second method for delineating the portion of the image used for calculating the threshold was to use morphological filtering on the FLAIR cerebral tissue mask. A sequence of morphological filters was applied to the mask to erode the surface. The surfaces of the ventricles were excluded from this erosion by filling them in while the erosion filters were being applied. The voxels eroded from the cerebral tissue mask were used to form a new mask. Four sequences of erosion filters were applied to the cerebral tissue mask resulting in four variations of a peripheral tissue mask.

The third method for delineating a region of brain for threshold calculation was to use the peripheral mixed tissue image described above. The peripheral mixed tissue mask includes voxels from the periphery of the cerebral tissue that have a probability between 0% and 50% of being white matter. These methods resulted in six different portions of the image to choose from when setting the threshold value.

Applying a single threshold to all cerebral tissue causes many voxels to be included in the WMH burden estimate which are not located in white matter. Four basic

approaches were tried for defining the portion of the image to which the threshold was applied. The first approach was to use the cerebral white matter mask described above. That would limit detection of WMH to voxels located in the white matter. However, errors in the segmentation of the MPRAGE image occasionally resulted in important areas of the white matter being excluded from the white matter mask.

The second approach to defining the WMH search area was to erode the surface of the cerebral tissue mask. The surfaces of the ventricles were excluded from the erosion process by temporarily filling in the ventricles. Eroding the surface removed most of the voxels containing gray matter. Four sequences of erosion filters were applied to the cerebral tissue mask resulting in four variations of the mask for excluding the cerebral surface tissue. The different degrees of erosion removed different amounts of the gray matter. Larger degrees of erosion also removed large portions of the white matter, increasing the probability of missing WMH. The erosion filters were applied to the cerebral mask generated from the MPRAGE image which were then spatially transformed to be registered with the FLAIR image. The erosion filters were applied to MPRAGE masks rather than to FLAIR mask because the MPRAGE voxels were more isometric than the FLAIR voxels.

The third approach to defining the WMH search area was to modify the cerebral white matter mask by adding all cerebral tissue voxels in the central portion of the brain. This provided a way to search for WMH in some white matter tissue which had been misclassified as gray matter. The exclusion of misclassified voxels in the periphery was not corrected.

The final approach for defining the search area for WMH was to use two threshold values on different delineations of the search area. One threshold was applied to the cerebral white matter image. A higher threshold was then applied to the cerebral tissue image. The misclassified white matter was generally very hyperintense. The

higher threshold included the WMH from misclassified white matter while most of the hyperintense gray matter was still less intense than this higher threshold.

These approaches generated six different portions of the FLAIR image to choose from for limiting the WMH search. The forth approach also added the extra dimension of a second threshold.

2.4 Selection of Parameter Values for WMH Burden Estimation

The best measurement of this algorithm's accuracy would have been one which compared the estimated WMH burden with the actual WMH burden for many images. Algorithm refinement would have then proceeded by adjusting the parameter values to maximize the accuracy of the WMH burden estimate. However, measurements of the WMH burden for the images used in this study were not available. A measurement of WMH burden that was available for many of the images was a subjective measurement which rated the WMH burden as "Normal", "Minimal", "Moderate", or "Advanced".

A subset of the images available from the Dallas Heart Study were used as a training set for algorithm refinement. The training set consisted of images from 161 subjects for which subjective ratings of the WMH burden had been made. The WMH burden was rated as "Normal" for 67 images, "Minimal" for 66 images, "Moderate" for 21 images, and "Advanced" for 7 images. One of the "Advanced" images had been acquired on a different scanner from all the other images so it was not used in this study. Also, a processing error had occurred for one of the "Minimal" images so it was not used. Removing these images from the training set left 159 images. Figure 2.9 shows a plot of the training set images with the WMH burden estimate on the vertical axis and the subjective rating on the horizontal axis.

For each adjustment made to the algorithm parameters, a different relationship of WMH burden estimate to subjective rating was produced. The refinement of the

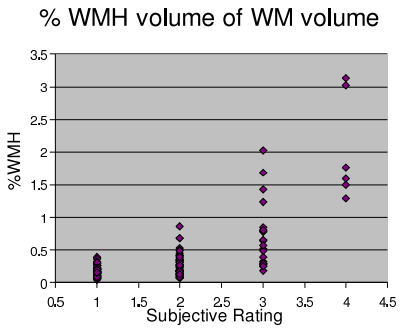

Figure 2.9. WMH Burden Estimates
for the Training Set Images.

algorithm required comparing the accuracy of the algorithm for many parameter settings. The parameters were used to select the threshold calulation method, a threshold scaling factor, and the threshold application regions. WMH burden estimates were calculated for each combination of these parameters. A graphical representation of the algorithm results is not very helpful in discerning which set of parameter values gives the best results. Figure 2.10 plots the results of the algorithm using 18 sets of parameter values to illustrate the difficulty of comparing the results visually.

In order to compare the WMH burden estimates with the subjective ratings, the WMH burden estimates were quantized to four values. Three approaches to setting the breakpoints for quantizing the WMH burden estimate were explored.

The first approach was to estimate the mean and standard deviation of the WMH burden estimate for an image at each subjective rating. The mean and standard deviation was estimated from the WMH burden estimate of the available images. The breakpoints were set at the values where adjacent subjective ratings had equal likelihood of occurring.

The second approach was to calculate the cumulative distribution for the images assigned to each subjective rating. The cumulative distribution was calculated at 100

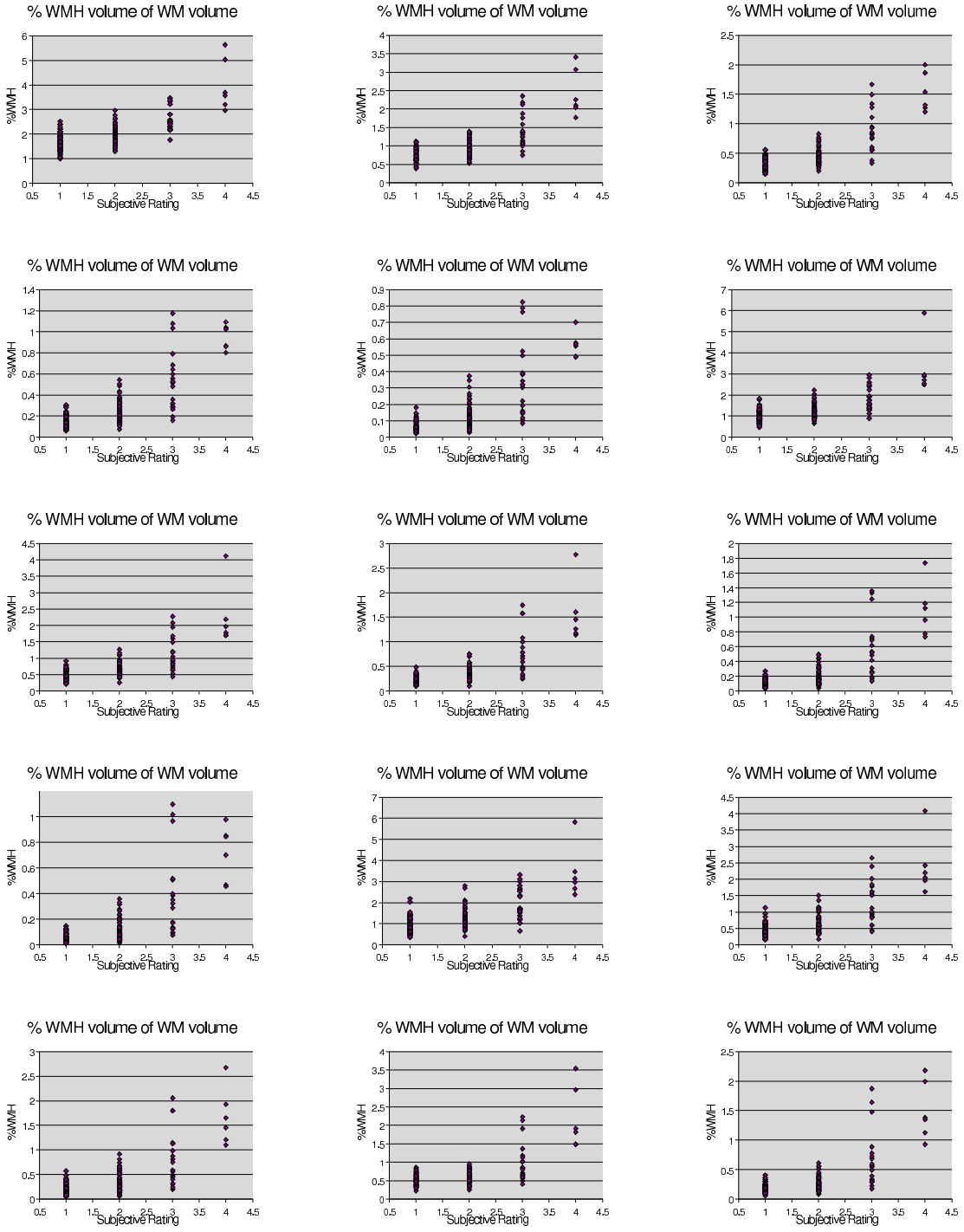

Figure 2.10. 18 Sets of WMH Burden Estimates for the Training Set Images.

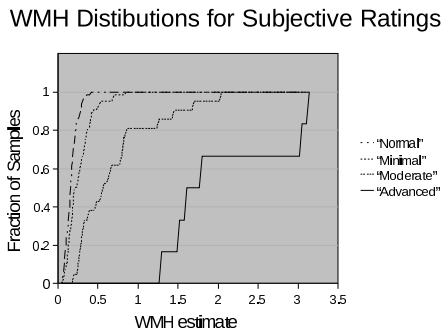

Figure 2.11. Distributions of WMH Burden Estimates for Setting Breakpoints.

evenly spaced values between the minimum and maximum WMH burden estimates for all the images in the training set. The distributions of adjacent subjective ratings were compared and the value where the largest difference between the distributions occurred was selected as a quantization breakpoint. A graph of the cumulative distributions of the results using one of the sets of parameter values is given in Figure 2.11.

The final approach to setting breakpoints was to use an ROC type analysis. For each breakpoint, a two column, two row table was constructed. The images with a subjective rating below the breakpoint being considered were placed in the right column of the table and the other images were placed on the left. Each table was tested at 100 threshold values evenly spaced between the minimum and the maximum WMH burden estimates for all the images. The images with a WMH burden estimate above the threshold being tested were placed in the top row of the table and other images were placed in the bottom row.

The upper left cell represents true positive (TP) WMH burden estimates. The lower right cell represents true negative (TN) WMH burden estimates. The upper right cell represents false positive (FP) WMH burden estimates (Type I error). The

Table 2.1. A Typical Error Matrix for the Training Set of Images.

	Rating 1	Rating 2	Rating 3	Rating 4
Quantized 1	57	33	1	0
Quantized 2	10	26	7	0
Quantized 3	0	6	10	0
Quantized 4	0	0	3	6

lower left cell represents false negative (FN) WMH burden estimates (Type II error). The threshold for WMH burden estimate which produced the greatest difference between the true positive rate ($\frac{TP}{TP+FN}$) and the false positive rate ($\frac{FP}{FP+TN}$) for a given subjective rating breakpoint was selected as a quantization breakpoint.

The degree of agreement between the quantized WMH burden estimates and the subjective ratings was quantified by calculating the kappa coefficient.[5] This provided an objective way to compare the quantization breakpoints produced by the three methods described above. It also provided the means to evaluate the impact on the accuracy of the WMH burden estimation as the algorithm parameters were adjusted. The error matrix used to calculate kappa was a square matrix with four columns for the subjective ratings and four rows for the quantized WMH burden estimate. The number of images assigned to each cell was recorded in the cell. The error matrix for one set of parameter values is given in Table 2.1.

The actual agreement in the table was calculated by dividing the number of images for which the quantized WMH burden estimate agreed with the subjective rating by the total number of images. The expected agreement due to chance was calculated by multiplying the total number of images in a row by the total number of images in the corresponding column, then adding the four products and divid-

ing the result by the square of the total number of images. The kappa coefficient was calculated by taking the difference between the actual and expected agreement, and normalizing the result by the difference between 1 (perfect agreement) and the expected agreement. $\kappa = \frac{Pr(a)-Pr(e)}{1-Pr(e)}$.

At the time of this study the magnitude of the error in the WMH burden estimates and the magnitude of the error in the subjective ratings were not known. It was assumed, however, that these errors were independent, so it was also assumed that closer agreement of the quantized WMH burden estimate with the subjective rating would indicate closer agreement of the WMH burden estimate with the actual WMH burden.

The kappa coefficient was calculated for WMH burden estimates generated using sets of parameter values to select each method of calculating the quantization breakpoints, each method of threshold calculation, and each method of delineation of hyperintensity search region. However, the set of parameter values to use for calculating WMH burden was not selected solely on the basis of the kappa coefficient. Subjective factors, such as visual comparisons of the selected WMH voxels with the FLAIR image, were used in conjunction with the kappa coefficients to select which set of algorithm parameter values to use for the rest of the study.

Once the parameter values for the WMH burden estimation algorithm were selected, a plot was made of the WMH burden estimate against the subjective ratings for the training set of images. Outliers were identified and adjusted if deemed appropriate.

2.5 Evaluation of the WMH Burden Estimation Algorithm

After the parameters of the WMH burden estimation algorithm were set through the algorithm refinement process, the agreement between the WMH burden estimate

and the subjective rating was evaluated using a test data set. The test set was a subset of the Dallas Heart Study data collected on the same equipment as the training set, but using different subjects. There were a total of 247 images which were rated on the same subjective scale as the images in the training set. All ratings in this study were made by the same observer. The intra-rater repeatability of the measures was not tested and the images of the test set were all rated after the training set had been rated. No estimates were available for bias drift in the ratings or for changes in rating variance over time. The WMH burden was rated as "Normal" for 114 images, "Minimal" for 97 images, "Moderate" for 28 images, and "Advanced" for 8 images. One of the "Advanced" images had an apparent processing error. The reason for the anomalous result has not been determined but the image was exclude from the test.

The kappa coefficient was calculated for the evaluation of the degree of agreement between the WMH burden estimates and the subjective ratings. The kappa coefficient was first used to determine whether the agreement of the WMH burden estimates and the subjective ratings for the test set was greater than would have been expected for random chance. The kappa coefficient was then used to determine if the degree of agreement was less than the degree of agreement demonstrated with the training set at a P value of 0.05.

WMH burden has been correlated with several biomarkers, many of which were included in the Dallas Heart Study database. The relationship between the WMH burden estimate and several biomarkers was investigated to determine if the correlation reported in the literature could be demonstrated using this WMH burden estimation algorithm. The data analysis used to investigate these correlations varied according to the nature of the data collected for the biomarkers.

The first correlation tested was the correlation of the WMH burden estimate with age. A positive correlation between age and WMH burden has been demonstrated.[6]

The age of each subject was calculated for the day of their MRI scans. The approach taken here was to perform a regression on the data. Age was taken as the independent variable with WMH burden estimate was the dependent variable. The F value of the ANOVA for the regression was tested to determine if the slope determined by the regression were positive at a P value of 0.05.

The second correlation tested was the correlation of the WMH burden estimate and a diagnosis of hypertension. A positive correlation between WMH burden and hypertension has been shown.[7] Data for hypertension in the the Dallas Heart Study subjects was available for previous visits several years ago. A more recent assessment of hypertension in these subjects was not available at the time of this report. The WMH burden estimates were grouped by diagnosis of hypertension and a t test at a P value of 0.05 was performed to determine whether the group with a previous diagnosis of hypertension had a larger WMH burden estimate than the group not diagnosed as hypertensive at the earlier time.

The third correlation tested was between the WMH burden estimate and a diagnosis of diabetes. A positive correlation between WMH burden and diabetes has been shown.[8] Again, data for diabetes in the the Dallas Heart Study subjects was available for previous visits, but a more current assessment was not available at the time of this report. The WMH burden estimates were grouped by diagnosis of diabetes and a t test at a P value of 0.05 was performed to determine whether the group with a previous diagnosis of diabetes had a larger WMH burden estimate than the group not diagnosed as diabetic at the earlier time.

The fourth correlation tested was between WMH burden estimate and cognitive ability as measured by the MOCA test.[9] A negative correlation between WMH burden and cognitive ability has been shown.[10] MOCA scores were reported on a discrete scale of 0 to 30. A regression was performed on the data using MOCA score

as the independent variable and WMH burden estimate as the dependent variable. The F value of the ANOVA for the regression was tested to determine if the slope determined by the regression was negative at a P value of 0.05.

Tests for correlations of the WMH burden estimate with gender and with ethnicity were also performed. The test used with gender was a t test with a P value of 0.05. The test used with ethnicity was ANOVA followed by two-tailed Tukey multiple comparison tests. The P value set for each was 0.05.

To remove the effect of interactions between the biomarkers and age, the WMH burden estimate was corrected for age using the slope and intercept calculated by the linear regression. The same tests for correlation with the biomarkers were then repeated using the residuals from the regression with age. For the comparison with MOCA scores, a regression of WMH burden estimate was performed against both age and MOCA scores.

CHAPTER 3

RESULTS

3.1 Selection of Parameter Values for WMH Burden Estimation

The WMH burden was estimated for each of the 159 images in the training set. The estimation was recalculated for each of 213 sets of parameter values. The three quantization methods were applied to the results of each set of parameter values and a kappa coefficient was computed for each. This provided a measure of the agreement between the quantized WMH burden estimates and the subjective ratings for each set of parameter values.

The first decision in the refinement process was the selection of the quantization method to use in calculating the kappa coefficient. The differences between the kappa coefficients for the quantization methods were calculated for each set of parameter values. The means and standard deviations of the differences are reported in Table 3.1. The second quantization method produced the greatest kappa coefficients, although it is not significantly different from the third method. The second method was selected as the method to use for quantizing the WMH burden estimate.

Table 3.1. Comparison of Kappa Coefficients for Quantization Methods

Pairwise Differences	Method 1 vs. Method 2	Method 1 vs. Method 3	Method 2 vs. Method 3
Mean	-0.10	-0.07	0.03
Standard Deviation	0.06	0.06	0.03

The kappa coefficient of 0.48 was produced using the cerebral tissue voxels for the threshold calculation, 4.5 standard deviations above the mean as the threshold level, and the peripheral white matter and central tissue portions of the image as the region to apply the threshold to. This kappa coefficient was the largest one produced without making adjustments for outliers.

The relative accuracy of the WMH burden estimation produced using different sets of parameter values was evaluated subjectively by displaying the FLAIR images side by side with and without WMH overlays. This comparison was made for several sets of parameter values which produced kappa coefficients which were not statistically less than the largest kappa coefficient obtained. The set of parameter values that was selected was chosen because it did not require the use of morphological filters and it accounted for misclassified tissue from the whole cerebrum rather than just the central portion of the cerebrum.

The selected set of parameter values used the peripheral mixed tissue for computing the thresholds. Two threshold values were used, a lower threshold value that was 3.0 standard deviations above the mean and a higher threshold value that was 3.5 standard deviations above the mean. The lower threshold was applied to the cerebral white matter image. The resulting mask was combined with a mask generated by applying the higher threshold to the cerebral tissue image.

The kappa coefficient computed for the agreement of the WMH burden estimates with the subjective ratings using this set of parameter values was 0.40 as shown in Table 3.2. The 95% confidence interval for this kappa coefficient is 0.28 to 0.53 which includes the value 0.48 which was the largest value of kappa obtained for a set of parameter values.

A plot of the WMH burden estimate for the images against the subjective ratings revealed that three images that were rated as “Moderate” had much higher

Table 3.2. Error Matrix and Kappa Coefficient for the Training Set of Images

	Rating 1	Rating 2	Rating 3	Rating 4	Totals	Totals
Quantized 1	57	33	1	0	91	0.57
Quantized 2	10	26	7	0	43	0.27
Quantized 3	0	6	10	0	16	0.10
Quantized 4	0	0	3	6	9	0.06
Totals	67	65	21	6	159	
Totals/all	0.42	0.41	0.13	0.04		

PR(a)	0.62	
PR(e)	0.37	
kappa	0.40	±0.12

WMH burden estimates than the other images with that rating. A visual review of the three images indicated that the WMH burden of these images was more similar to images rated "Advanced" than to those rated "Moderate". For the purpose of setting the breakpoints used to quantize the WMH burden estimate, these three images were recategorized as "Advanced". Changing those three ratings increased the kappa coefficient for the agreement of the WMH burden estimates with the subjective ratings from 0.40 to 0.43.

Another effect of changing those three ratings was to adjust the breakpoints used to quantize the WMH burden estimate. The breakpoints derived using the second quantization method were recorded for later use in comparing the WMH burden estimation results using the selected set of parameter values to the subjective ratings for the test data set.

Table 3.3. Error Matrix and Kappa Coefficient for the Test Set of Images

	Rating 1	Rating 2	Rating 3	Rating 4	Totals	Totals
Quantized 1	97	44	1	0	142	0.58
Quantized 2	15	50	12	0	77	0.31
Quantized 3	2	3	13	1	19	0.08
Quantized 4	0	0	2	6	8	0.03
Totals	114	97	28	7	246	
Totals/all	0.46	0.39	0.11	0.03		

PR(a)	0.67	
PR(e)	0.40	
kappa	0.46	±0.10

3.2 Evaluation of the WMH Burden Estimation Algorithm

The WMH burden was estimated for the 246 images of the test data set using the selected set of parameter values for the WMH burden estimation algorithm. The kappa coefficient for the agreement between the WMH burden estimate and the subjective ratings was 0.46 with a variance of 0.0025. The error matrix and kappa coefficient are given in Table 3.3. This is significantly different from a random distribution at a P value of 0.05. The kappa and variance calculated for the training set were 0.43 and 0.0040 respectively. The kappa coefficients for the training and test data sets were not different at a P value of 0.05.

The images in the training data set which were used for algorithm refinement were included in tests for correlations between biomarkers and the WMH burden estimate. The WMH burden estimate was calculated for 1003 images. Age and

Table 3.4. Significance of Various Factors on WMH Burden

Factor	Analysis Type	Significant at P value of 0.05	
		Comparing %WMH	Comparing Age Adjusted %WMH
Age	Regression	yes	N/A
MOCA	Regression	yes	yes
Gender	t test	yes	yes
Hypertension	t test	yes	yes
Diabetes	t test	yes	no
Ethnicity	ANOVA	yes	yes

gender data were available for 1003 images, ethnicity data and diagnoses of diabetes data were available for 973 images, diagnoses of hypertension data were available for 942 images, and MOCA scores were available for 236 images. The results from statistical tests of factors described below are presented in Tables 3.4 through 3.6.

A linear regression was calculated for the WMH burden estimate as a function of age. The slope was 0.018 and the intercept was -0.57. The r^2 of the regression was 0.139 and the regression was significant at a P value of 0.05.

A linear regression was calculated for the WMH burden estimate as a function of MOCA score. The slope was -0.013 and the intercept was 0.61. The r^2 of the regression was 0.024 and the regression was significant at a P value of 0.05. To take into account the interdependence of the MOCA score and age, a regression of the WMH burden estimate was performed with both age and MOCA scores. In this case, the r^2 was 0.12 and the MOCA factor was significant at a P value of 0.05.

Table 3.5. An ANOVA of the Age Adjusted WMH Burden by Ethnic Group

Group	Number	Average
Non-Hispanic Black	423	0.06
Non-Hispanic White	417	-0.05
Hispanic	113	-0.03
Other	20	-0.12

Source of variance	SS	df	MS
Within groups	184.98	969	0.19
Between groups	2.87	3	0.96
Total	187.85	972	

Analysis Statistic	Value
F	5.02
P value	0.0019

The average WMH burden estimate for females was 0.38 and the average for males was 0.32. The results of a t test showed that the difference was significant at a P value of 0.05. When the correction for age was included, the difference was still significant at 0.05. The averages for groups compared with t tests and the 95% confidence intervals are given in Table 3.6.

The average WMH burden estimate for diabetics was 0.54 and the average for non-diabetics was 0.34. The results of a one sided t test showed that the higher average WMH burden estimate for diabetics was significant at a P value of 0.05. When the correction for age was included the diabetes factor was not significant at a P value of 0.05.

Table 3.6. Average WMH Burden for Subjects of Various Groups

Characteristic of Group	Number of Subjects in Group	Average %WMH (95% confidence)	Average Age Adjusted %WMH (95% confidence)
Male	450	0.32(±0.06)	-0.04(±0.05)
Female	553	0.38(±0.06)	0.03(±0.05)
Hypertensive	259	0.57(±0.07)	0.11(±0.06)
Non Hypertensive	683	0.28(±0.07)	-0.04(±0.06)
Diabetic	76	0.54(±0.11)	0.06(±0.10)
Non Diabetic	897	0.34(±0.11)	0.00(±0.10)

The average WMH burden estimate for individuals diagnosed with hypertension was 0.57 and the average for non-hypertensive individuals was 0.28. The results of a one sided t test showed that the average WMH burden estimate for hypertensive individuals was greater at a P value of 0.05. When the correction for age was included the increase was still significant at 0.05.

The ethnicity of the subjects was reported as “Non-Hispanic Black”, “Non-Hispanic White”, “Hispanic”, or “Other”. There were 423 “Non-Hispanic Black”, 417 “Non-Hispanic White”, 113 “Hispanic”, and 20 “Other” subjects. The F value from an analysis of variance was 6.02 with 3 degrees of freedom in the numerator and 969 degrees of freedom in the denominator. The result was significant at a P value of 0.05. When the correction for age was included, the ethnicity factor was still significant at a P value of 0.05.

The Tukey multiple comparisons test yielded ambiguous results. The “Non-Hispanic Black” category had the greatest average WMH burden estimate which was 0.43, the “Non-Hispanic White” category had an average of 0.33, the “Hispanic”

category had an average of 0.26, and the "Other" category had the smallest average WMH burden estimate which was 0.21. The comparison between "Non-Hispanic Black" and "Other" indicated that the means of these categories were not different. Since no difference was found between the greatest and the least means, tests between the other means should not be performed with the Tukey multiple comparison tests. However, a t test between the means of "Non-Hispanic Black" and "Non-Hispanic White" indicated that the means were significantly different at a P value of 0.05.

CHAPTER 4

DISCUSSION

A reliable and sensitive algorithm was developed for estimating the WMH burden from pairs of MPRAGE and FLAIR images. This fully automated algorithm did not require any operator review of the for the 1006 images used in this study.

The algorithm was tested to determine if the WMH burden estimate generated by the algorithm were correlated with known risk factors for WMH burden. The results showed expected correlations with age, reduced cognitive function, hypertension, and gender. Ethnicity was also shown to be a significant factor, but the statistical tests proposed before data analysis was performed were not able to determine which of the ethnicity groupings were different.

The possibility of interdependency between age and the other factors was taken into account. Conclusive results were not obtained for diabetes. The small number of diabetics among the subjects may have prevented finding a definitive conclusion.

APPENDIX A

SOFTWARE MANUAL

A.1 DHS2 MRI Image Database

The DICOM files for the DHS2 MRI images are accessed through the server named "massive.swmed.edu". The scripts included in this appendix assume that the directory on this server containing the files and sub-directories for this data is mounted as "/mnt/dhs2mri/".

The information necessary for locating files for specific MRI scans of specific patients is contained in the SQL database DicomIDB2 located on the server "massive.swmed.edu". This database is used by scripts in this appendix for accessing other necessary patient information as well.

The image and data files generated by the scripts in this appendix are written to the local hard drive and later transferred to the server. This protocol is used as a work around in order to set file permissions as read/write rather than read only. Appropriate permissions can be obtained by copying the files from the local directory through the server "radteach.swmed.edu" to the desired directory using the Linux command "scp".

A.2 Selection of Data to Process

The first task in processing the DHS2 MRI data is to select the patient identifiers (MRNs) for which the data is to be processed. Several of the scripts require a list of the MRNs that are to be processed. The required format is a text file with one 8 digit MRN per line.

The script file "collect_mrns_by_date" selects MRNs of patients whose MPRAGE scans were inserted into the database after the interactively adjustable start date but not after the interactively adjustable stop date. The 8 digit MRNs are output to a text file. The call for the program is "bash collect_mrns_by_date output_filename".

The start and stop dates are requested during the interactive portion of the script. The date format accepted by the script is "yyyymmdd".

A.3 Parallel Processing

Due to the large number of images to be processed and the long run-times of some of the programs, it is desirable to make use of parallel processing. The data processing scripts listed in this appendix read MRNs from the standard input device and complete the processing of data for one MRN before moving on to process data for the next MRN. A separate script is required to simultaneously utilize the 8 processors available on the computer used for this project. The script "parallel_7" takes as input the file name of a "processing script" and the file name of a file containing the MRNs to be processed. The MRNs are divided into seven groups and written to separate files which will be used as input to the next step.

Seven instances of the "processing script" are initiated simultaneously with the 7 MRN files used as input to these instances. In this way, seven processors are simultaneously utilized for image processing while the 8th processor is left underutilized to provide reasonable system response. The 7 separate MRN files are named "parallel_7_processing_script_filename_groupN.mrn", with "processing_script_filename" replaced with the filename of the "processing script" and the "N" of "groupN" replaced with the MRN group number which ranges from 1 to 7. The standard output generated by the "processing script" is written to a file named "processing_script_filename_1.output", with "processing_script_filename" replaced by the filename of "processing script" and "N" replaced by the group number which ranges from 1 to 7.

A.4 Image Processing Pipeline

The image processing pipeline is implemented in the script "WMH_estimate". The output files produced for each MRN is written to a directory created using the MRN as its directory name. The script can be called with a file of MRNs as input by typing "cat mrn_filename | bash WMH_estimate output_filename", where "mrn_filename" is the name of a file containing the MRNs of the images to be processed and "output_filename" is the name for the output normally directed to the standard output device.

The pipeline begins by locating and reformatting the MPRAGE image and the FLAIR image for a given MRN. The FSL routine SIENAX is used to segment the MPRAGE image and to generate a matrix defining the spatial transformation require to register the MNI152 brain atlas to the MPRAGE image. Masks generated from the appropriate classes of the MNI152 brain atlas are used to crop the CSF, white matter and gray matter probability maps generated by SIENAX. The resulting masks represent cerebral CSF, cerebral gray matter and cerebral white matter. These probability maps are used to make binary masks for cerebral tissue, cerebral white matter, and cerebral periphery mixed tissue.

The masks are then spatially transformed to be registered with the FLAIR image. The matrix used to define this transformation is generated using a normalized mutual information cost function in registering the MPRAGE image to the FLAIR image. The masks are applied to the FLAIR image to produce FLAIR images of the specified tissues. Image statistics collected from cerebral periphery mixed tissue are used to generate threshold values to be applied to the FLAIR images of cerebral white matter and cerebral tissue. A binary mask is generated of the voxels which either have white matter intensities that exceed the lower threshold or cerebral tissue

intensities that exceed the upper threshold. The resulting WMH mask is written to disk.

The script named "collect_WMH_estimate" is used to calculate the percentage of the brain's total white matter that is hyperintense. Files in the MRN output directory are used to calculate the WMH volume. The total white matter volume as estimated by SIENAX is read from the file "report.sienax". The voxel dimensions for the MPRAGE image and the FLAIR image are read from the DICOM headers on server containing the DHS2 MR images. Finally, the patient's birth date, the patient's gender, and the date of the study are collected from the SQL database. This information is written to the standard output device as one line of data per MRN.

A.5 Linux Scripts

The scripts described above are presented below.

collect_mrns_by_date (page 1 of 4)

```
if test "_$1" = "_" ; then
  echo "supply filename for mrns";
  exit;
fi;
#########################################################
### Select dates for mrn selection
#########################################################

study_start_date="20070901";
        ### Studies before this date will be excluded
last_brain_vol_date="20070901";
        ### Studies before this date have previously been processed
yesterday=`date -d"yesterday" '+%Y%m%d'`;
test $last_brain_vol_date -lt $study_start_date && last_brain_vol_date=
        $study_start_date;
test $last_brain_vol_date -gt $yesterday && last_brain_vol_date=$yesterday;
start_date=$last_brain_vol_date;
end_date=$yesterday
```

collect_mrns_by_date (page 2 of 4)

```
echo -n -e\n "\nAll entries since $start_date through $end_date will be selected.\nPress
        ENTER key to accept starting date or enter a new starting date. ";
read new_date;
while test ! ${#new_date} = "0" && test $new_date != $start_date; do
        if test ${#new_date} = "8" -a ${new_date%[^0-9]*} = $new_date && test
        $new_date -ge $study_start_date -a $new_date -lt $yesterday; then
                start_date=$new_date;
        else
                echo -e\n "\n****Invalidate starting date. Enter a date from
        $study_start_date but before $yesterday.***\n****Only mrns after this date will
        be selected.****\n"
        fi;
        echo -n -e\n "\nAll entries since $start_date through $end_date will be
        selected.\nPress ENTER key to accept starting date or enter a new starting date. ";
        read new_date;
done;
echo -n -e\n "\nAll entries since $start_date through $end_date will be selected.\nPress
        ENTER key to accept ending date or enter a new ending date. ";
```

collect_mrns_by_date (page 3 of 4)

```
read new_date;
while test ! ${#new_date} = "0" && test $new_date != $end_date; do
        if test ${#new_date} = "8" -a ${new_date%[^0-9]*} = $new_date && test
        $new_date -gt $start_date -a $new_date -le $yesterday; then
                end_date=$new_date;
        else
                echo -e\n "\n****Invalidate ending date. Enter a date after $start_date up
        through $yesterday.****\n****Only mrns up through this date will be
        selected.****\n"
        fi;
        echo -n -e\n "\nAll entries since $start_date through $end_date will be
        selected.\nPress ENTER key to accept ending date or enter a new ending date. ";
        read new_date;
done;
echo "";

#########################################################################
### Query database for MRN's of studies included between specified dates
```

collect_mrns_by_date (page 4 of 4)

```
#########################################################################

echo "select PatParent from StudyLevel,SeriesLevel where SeriesLevel.SerDes like
        '%MPRAGE%' AND SeriesLevel.StuParent=StudyLevel.StuInsUID AND
        StuDat>=$study_start_date AND SeriesLevel.InsertDate>$start_date AND
        SeriesLevel.InsertDate<=$end_date;" |
mysql -uxxx -pxxxx -h massive.swmed.edu DicomIDB2 | grep "\b[7,9][[:digit:]]\{7\}\b">
        $1
```

parallel_7 (page 1 of 4)

```
script_name=`echo $1`;
mrn_name=`echo $2`;
mrn_count=(`wc ./$mrn_name`);
mrn_count_7=`echo "0 k ${mrn_count[0]} 7 / p"|dc -`;
mrn_count1=`dc -e "0 k ${mrn_count[0]} $mrn_count_7 7 * - 6 + 7 / $mrn_count_7 +
        p"`;
mrn_count2=`dc -e "0 k ${mrn_count[0]} $mrn_count_7 7 * - 5 + 7 / $mrn_count_7 +
        p"`;
mrn_count3=`dc -e "0 k ${mrn_count[0]} $mrn_count_7 7 * - 4 + 7 / $mrn_count_7 +
        p"`;
mrn_count4=`dc -e "0 k ${mrn_count[0]} $mrn_count_7 7 * - 3 + 7 / $mrn_count_7 +
        p"`;
mrn_count5=`dc -e "0 k ${mrn_count[0]} $mrn_count_7 7 * - 2 + 7 / $mrn_count_7 +
        p"`;
mrn_count6=`dc -e "0 k ${mrn_count[0]} $mrn_count_7 7 * - 1 + 7 / $mrn_count_7 +
        p"`;
echo "Total mrns to process = ${mrn_count[0]}";
echo "Number of mrns to pipe to each process = $mrn_count_7";
```

parallel_7 (page 2 of 4)

```
cat $mrn_name|
(
 for ((i=1;i<=mrn_count1;i++)); do
   read mrn;
   echo $mrn;
 done>parallel_7_${script_name}_group1.mrn;
 bash $script_name<parallel_7_${script_name}_group1.mrn>&$
          {script_name}_1.output&
 for ((i=1;i<=mrn_count2;i++)); do
   read mrn;
   echo $mrn;
 done>parallel_7_${script_name}_group2.mrn;
 bash $script_name<parallel_7_${script_name}_group2.mrn>&$
          {script_name}_2.output&
 for ((i=1;i<=mrn_count3;i++)); do
   read mrn;
   echo $mrn;
 done>parallel_7_${script_name}_group3.mrn;
```

parallel_7 (page 3 of 4)

```
bash $script_name<parallel_7_${script_name}_group3.mrn>&$
        {script_name}_3.output&
for ((i=1;i<=mrn_count4;i++)); do
  read mrn;
  echo $mrn;
done>parallel_7_${script_name}_group4.mrn;
bash $script_name<parallel_7_${script_name}_group4.mrn>&$
        {script_name}_4.output&
for ((i=1;i<=mrn_count5;i++)); do
  read mrn;
  echo $mrn;
done>parallel_7_${script_name}_group5.mrn;
bash $script_name<parallel_7_${script_name}_group5.mrn>&$
        {script_name}_5.output&
for ((i=1;i<=mrn_count6;i++)); do
  read mrn;
  echo $mrn;
done>parallel_7_${script_name}_group6.mrn;
```

parallel_7 (page 4 of 4)

```
bash $script_name<parallel_7_${script_name}_group6.mrn>&$
        {script_name}_6.output&
while read mrn;do
  echo $mrn;
done>parallel_7_${script_name}_group7.mrn;
bash $script_name<parallel_7_${script_name}_group7.mrn>&$
        {script_name}_7.output&
)
```

WMH_estimate (page 1 of 11)

```
#####################################################
### Initial setup
#####################################################

### Keep AFNI from checking for new versions
AFNI_VERSION_CHECK=NO ; export AFNI_VERSION_CHECK;
### Set pointers for root directories
root_dir="/home/keith/dhs2/processed_data/";
        ### Root directory for processed image and collateral data
periph=/usr/local/fsl/data/standard/MNI152_T1_2mm_strucseg_periph;
        ### MNI mask of peripheral cortex
mask=/mnt/dhs2mri/keith/dhs2/mni152
        ### Directory of MNI masks

#########################################################################
### Process MRI data for MRN's
#########################################################################
```

WMH_estimate (page 2 of 11)

```
while read mrn ;do
  echo "Processing images from MRN: $mrn";
  mrn_dir=$root_dir$mrn;
  mprage=${mrn_dir}/${mrn}_mprage;
  flair=${mrn_dir}/${mrn}_flair;



################################
### Get mprage image

  image_type_string=\'%MPRAGE%\';
  echo "select PatParent,SerInsUID from StudyLevel,SeriesLevel where
        SeriesLevel.SerDes like $image_type_string AND
        SeriesLevel.StuParent=StudyLevel.StuInsUID AND PatParent=$mrn;" |
    mysql -uxxxx -pxxxx -h massive.swmed.edu DicomIDB2 |
    while read PatParent SerInsUID;do
        test ${#PatParent} = "8" -a ${PatParent%[^0-9]*} = $PatParent && test $
```

WMH_estimate (page 3 of 11)

```
      {PatParent:0:1} -eq "7" -o ${PatParent:0:1} -eq "9"  && ls -R /mnt/dhs2mri/
      $PatParent |
        grep "$SerInsUID"|
          while read dirname;do
                if test ${dirname: -1} = ":" ; then
                        echo  ${dirname%:};
                fi;
          done;
done|
  (read mprage_dir ;
   mrn=${mprage_dir#/*/*/};
   mrn=${mrn%%/*};
   dicom2afni $mprage_dir ${mrn_dir}/ ${mrn}_mprage;
   cd ${mrn_dir}/;
   3dresample -prefix ${mprage}_las -inset ${mrn}_mprage+orig -orient RPI;
   3dAFNItoNIFTI ${mrn}_mprage_las+orig;
   rm ${mrn_dir}/*+orig.*;
   mv ${mprage}_las.nii ${mprage}.nii;
```

WMH_estimate (page 4 of 11)

```
    gzip ${mprage}.nii;)

########################################
### Get flair image

 image_type_string=\'%FLAIR%\';
 echo "select PatParent,SerInsUID from StudyLevel,SeriesLevel where
        SeriesLevel.SerDes like $image_type_string AND
        SeriesLevel.StuParent=StudyLevel.StuInsUID AND PatParent=$mrn;" |
  mysql -uxxxx -pxxxx -h massive.swmed.edu DicomIDB2 |
  while read PatParent SerInsUID;do
        test ${#PatParent} = "8" -a ${PatParent%[^0-9]*} = $PatParent && test $
        {PatParent:0:1} -eq "7" -o ${PatParent:0:1} -eq "9"  && ls -R /mnt/dhs2mri/
        $PatParent |
          grep "$SerInsUID"|
            while read dirname;do
                if test ${dirname: -1} = ":" ; then
                        echo  ${dirname%:};
```

WMH_estimate (page 5 of 11)

```
                fi;
            done;
    done|
     (read flair_dir ;
      mrn=${flair_dir#/*/*/};
      mrn=${mrn%%/*};
      dicom2afni $flair_dir ${mrn_dir}/ ${mrn}_flair;
      cd ${mrn_dir}/;
      3dresample -prefix ${flair}_las -inset ${mrn}_flair+orig -orient RPI;
      3dAFNItoNIFTI ${mrn}_flair_las+orig;
      rm ${mrn_dir}/*+orig.*;
      mv ${flair}_las.nii ${flair}.nii;
      gzip ${flair}.nii;)

##############################################
### Run SIENAX on MPRAGE

 test -f $root_dir${mrn}/report.sienax && echo "Previous analysis overwritten for $mrn"
```

WMH_estimate (page 6 of 11)

```
        >> ${root_dir}repeated_brain_volume.txt;
  cd ${mrn_dir}/;
  sienax ${mrn}_mprage -o ${mrn_dir} -d -r -B "-d -v" -S "-v 5";

##############################################
### Generate cerebral WM image from FLAIR

### Mask out brainstem and cerebellum from the PVE of WM

  flirt -in ${mask}/cerebellar_mask -ref ${mprage} -applyxfm -init $
        {mrn_dir}/I2std_inv.mat -out ${mprage}_cerebellar_mask;
  fslmaths ${mprage}_cerebellar_mask -bin -mul -1 -add 1 $
        {mprage}_cerebellar_inv_mask;
  flirt -in ${mask}/brainstem_mask -ref ${mprage} -applyxfm -init $
        {mrn_dir}/I2std_inv.mat -out ${mprage}_brainstem_mask;
  fslmaths ${mprage}_brainstem_mask -bin -mul -1 -add 1 $
        {mprage}_brainstem_inv_mask;
  fslmaths ${mrn_dir}/I_stdmaskbrain_pve_0_segvent -thr .3 -add 1 -uthr 1 -bin $
```

WMH_estimate (page 7 of 11)

```
        {mprage}_vent_inv_mask -odt short;
  fslmaths ${mrn_dir}/I_stdmaskbrain -mas ${mprage}_cerebellar_inv_mask -mas $
        {mprage}_brainstem_inv_mask -mas ${mprage}_vent_inv_mask -bin $
        {mprage}_cerebral_mask;
  fslmaths ${mrn_dir}/I_stdmaskbrain_pve_2 -mas ${mprage}_cerebral_mask $
        {mprage}_cerebral_pve_2;

### Generate mask of cerebral tissue and cerebral WM
  fslmaths ${mrn_dir}/I_stdmaskbrain_pve_0 -thr .1 -add 1 -uthr 1 -bin -mas $
        {mprage}_cerebral_mask ${mprage}_cerebral_tissue_mask -odt short;
  fslmaths ${mprage}_cerebral_pve_2 -thr .5 -bin ${mprage}_cerebral_WM_mask -odt
        short;

### Generate an mask for Peripheral cotex in MPRAGE space
  flirt -in $periph -ref $mprage -out ${mprage}_periph_mask -applyxfm -init $
        {mrn_dir}/I2std_inv.mat
  fslmaths ${mprage}_periph_mask -bin ${mprage}_periph_mask;
```

WMH_estimate (page 8 of 11)

```
### Generate WM PVE image of peripheral cortex region.
  fslmaths ${mprage}_cerebral_pve_2 -mas ${mprage}_periph_mask -bin $
        {mprage}_cerebral_periph_WM_mask -odt short;
  fslmaths ${mprage}_cerebral_WM_mask -sub 1 -mul -1 -bin $
        {mprage}_cerebral_WM_inv_mask;
  fslmaths ${mprage}_cerebral_periph_WM_mask -mas $
        {mprage}_cerebral_WM_inv_mask ${mprage}_cerebral_periph_mixed_mask;

### Register the mprage cerebral mask, WM mask, and tissue mask to the FLAIR image

  flirt -in ${mprage} -ref ${flair} -out ${mprage}_resampled -omat $
        {mprage}_2_flair.mat -bins 256 -cost normmi -searchrx -5 5 -searchry -5 5
        -searchrz -5 5 -dof 12 -interp sinc -sincwidth 7 -sincwindow hanning;
### register the cerebral mask
  flirt -in ${mprage}_cerebral_mask -ref ${flair} -out ${flair}_cerebral_mask -applyxfm
        -init ${mprage}_2_flair.mat;
  fslmaths ${flair}_cerebral_mask -thr .5 -bin ${flair}_cerebral_mask -odt short;
  fslmaths ${flair} -mas ${flair}_cerebral_mask ${flair}_cerebral;
```

WMH_estimate (page 9 of 11)

```
### register the WM mask
  flirt -in ${mprage}_cerebral_WM_mask -ref ${flair} -out ${flair}_cerebral_WM_mask
        -applyxfm -init ${mprage}_2_flair.mat;
  fslmaths ${flair}_cerebral_WM_mask -thr .5 -bin ${flair}_cerebral_WM_mask -odt
        short;
  fslmaths ${flair} -mas ${flair}_cerebral_WM_mask ${flair}_cerebral_WM;
### register the cerebral tissue mask
  flirt -in ${mprage}_cerebral_tissue_mask -ref ${flair} -out $
        {flair}_cerebral_tissue_mask -applyxfm -init ${mprage}_2_flair.mat;
  fslmaths ${flair}_cerebral_tissue_mask -thr .5 -bin ${flair}_cerebral_tissue_mask -odt
        short;
  fslmaths ${flair} -mas ${flair}_cerebral_tissue_mask ${flair}_cerebral_tissue;
### register the cerebral peripheral mixed mask
  flirt -in ${mprage}_cerebral_periph_mixed_mask -ref ${flair} -out $
        {flair}_cerebral_periph_mixed_mask -applyxfm -init ${mprage}_2_flair.mat;
  fslmaths ${flair}_cerebral_periph_mixed_mask -thr .5 -bin $
        {flair}_cerebral_periph_mixed_mask -odt short;
  fslmaths ${flair} -mas ${flair}_cerebral_periph_mixed_mask $
```

WMH_estimate (page 10 of 11)

```
        {flair}_cerebral_periph_mixed;

################################################
### Estimate WMH volume

### Calculate WMH threshold using peripheral cerebral mixed

  mean_peri=`fslstats ${flair}_cerebral_periph_mixed -M`;
  std_peri=`fslstats ${flair}_cerebral_periph_mixed -S`;
  level30z_peri=`dc -e "5 k ${mean_peri} ${std_peri} 3.0 * + p"`;
  level35z_peri=`dc -e "5 k ${mean_peri} ${std_peri} 3.5 * + p"`;
################################################
### Apply threshold to data

  fslmaths ${flair}_cerebral_tissue -thr $level35z_peri -bin ${flair}_tissue_peri_thr35z
        -odt short;

  fslmaths ${flair}_cerebral_WM -thr $level30z_peri -bin ${flair}_WM_peri_thr30z -odt
```

WMH_estimate (page 11 of 11)

```
        short;

 fslmaths ${flair}_WM_peri_thr30z -add ${flair}_tissue_peri_thr35z -bin $
        {flair}_WM_30plus35 -odt short;

#################################################################
### Processing for current MRN complete-- go on to next

done;
```

collect_WMH_estimate (page 1 of 3)

```
pix_vol()
{
 echo "select PatParent,SerInsUID from StudyLevel,SeriesLevel where
       SeriesLevel.SerDes like $image_type AND
       SeriesLevel.StuParent=StudyLevel.StuInsUID AND PatParent=${mrn};" |mysql -
       uxxx -pxxx -h massive.swmed.edu DicomIDB2|grep -m 1 -e "${mrn}"|
(read -a uid;
 image_dir=`ls -R /mnt/dhs2mri/${mrn}/images |grep "${uid[1]}:"`;
 image_name=(`ls ${image_dir%:}`);
 pixel_dim=(`dcm_dump_file ${image_dir%:}/${image_name[5]}|grep -e "0018
       0088" -e "0028 0030"|sed s/[\\\]/" "/|sed s/[/][/]/" "/|sed s/[/][/]/" "/;`)
 dc -e "10 k ${pixel_dim[7]} ${pixel_dim[14]} * ${pixel_dim[15]} * p";)
}

patient_data()
{
 echo "select PatBirDat,StuDat,PatSex from PatientLevel,StudyLevel,SeriesLevel
       where SeriesLevel.SerDes like '%MPRAGE%' AND
```

collect_WMH_estimate (page 2 of 3)

```
        SeriesLevel.StuParent=StudyLevel.StuInsUID AND
        StudyLevel.PatParent=PatientLevel.PatID AND PatientLevel.PatID = ${mrn}"|
    mysql -uxxxx -pxxxx -h massive.swmed.edu DicomIDB2| grep -m 1 "[0-9]\{8\}";
   }

echo "mrn Voxel_scaling ICV_scaling mprage_pix_vol flair_pix_vol csf gm wm %brain
        birthdate study_date gender WM_30plus35z";

 while read mrn; do
   mrn_dir_2=/home/keith/dhs2/processed_data/${mrn}
   mrn_dir_1=/mnt/dhs2mri/keith/dhs2/processed_data/${mrn}
   flair_2=${mrn_dir_2}/${mrn}_flair;
   vscaling=(`cat ${mrn_dir_2}/report.sienax|grep -e "VSCALING"`);
   pixelsize=(`cat ${mrn_dir_2}/report.sienax|grep -e "Pixelsize"`);
   pixelscale=`dc -e "10 k ${pixelsize[2]} ${pixelsize[4]} * ${pixelsize[6]} * 1 / p" `;
   volumes=(`cat ${mrn_dir_2}/report.sienax|grep -e "Volumes"`);

   WM_30plus35z=(`fslstats ${flair_2}_WM_30plus35 -V`);
```

collect_WMH_estimate (page 3 of 3)

```
 image_type="'%MPRAGE%'";
 mprage_pix_vol=`pix_vol`;

 image_type="'%FLAIR%'";
 flair_pix_vol=`pix_vol`;

 patient_dat_array=`patient_data`;
 PatBirDat=${patient_dat_array[0]};
 StuDat=${patient_dat_array[1]};
 PatSex=${patient_dat_array[2]};

 echo $mrn $pixelscale ${vscaling[1]} $mprage_pix_vol $flair_pix_vol ${volumes[1]}
      ${volumes[2]} ${volumes[3]} ${volumes[4]} $PatBirDat $StuDat $PatSex $
      {WM_30plus35z[0]};
done;
```

REFERENCES

[1] B. Ovbiagele and J. L. Saver, "Cerebral white matter hyperintensities on mri: Current concepts and therapeutic implications," *Cerebrovasc Dis*, vol. 22, pp. 83–90, July 2006.

[2] M. Yoshita, E. Fletcher, and C. DeCarli, "Current concepts of analysis of cerebral white matter hyperintensities on magnetic resonance imaging," *Top Magn Reson Imaging*, vol. 16, pp. 399–407, Dec. 2005.

[3] S. M. Smith, M. Jenkinson, M. W. Woolrich, C. F. Beckmann, T. E. J. Behrens, H. Johansen-Berg, P. R. Bannister, M. DeLuca, I. Drobnjak, D. E. Flitney, R. Niazy, J. Saunders, J. Vickers, Y. Zhang, N. DeStefano, J. M. Brady, and P. M. Matthews, "Advances in functional and structural mr image analysis and implementation as fsl," *NeuroImage*, vol. 23(S1), pp. 208–219, Sept. 2004.

[4] R. W. Cox and J. S. Hyde, "Software tools for analysis and visualization of fmri data," *NMR in Biomedicine*, vol. 10, pp. 171–178, June 1997.

[5] R. G. Congalton and R. A. Mead, "A quantitative method of test for consistency and correctness in photointerpretation," *Photogrammetric Engineering and Remote Sensing*, vol. 49, pp. 69–74, Jan. 1983.

[6] P. C. Tumeh, A. Alavi, M. Houseni, A. Greenfield, T. Chryssikos, A. Newberg, D. A. Torigian, and G. Moonis, "Structural and functional imaging correlates for age-related changes in the brain," *Seminars in Nuclear Medicine*, vol. 37, pp. 69–87, Mar. 2007.

[7] D. Liao, L. Cooper, J. Cai, J. F. Toole, N. R. Bryan, R. G. Hutchinson, and H. A. Tyroler, "Presence and severity of cerebral white matter lesions and hy-

pertension, its treatment, and its control: The aric study," *Stroke*, vol. 27, pp. 2262–2270, Dec. 1996.

[8] H. Fukuda and M. Kitani, "Differences between treated and untreated hypertensive subjects in the extent of periventricular hyperintensities observed on brain mri," *Stroke*, vol. 26, pp. 1593–1597, Sept. 1995.

[9] Z. S. Nasreddine, N. A. Phillips, V. Bedirian, S. Charbonneau, V. Whitehead, I. Collin, J. L. Cummings, and H. Chertkow, "The montreal cognitive assessment, moca: A brief screening tool for mild cognitive impairment," *Journal of the American Geriatrics Society*, vol. 53, pp. 695–699, Apr. 2005.

[10] R. Au, J. Massaro, P. Wolf, *et al.*, "Association of white matter hyperintensity volume with decreased cognitive functioning: the framingham heart study," *Arch Neurol*, vol. 63, pp. 246–250, Feb. 2006.

BIOGRAPHICAL STATEMENT

Keith M. Hulsey was born in Gainesville, Georgia, in 1959. He received his B.S. degree in Engineering Physics from Cornell University, Ithaca, NY in 1981, his M.A. degree in Cross-Cultural Ministry from Dallas Theological Seminary, Dallas, TX in 1991 and his M.S. degree in Biomedical Engineering from The University of Texas at Arlington in 2008. From 1981 to 1989 he was with the Research and Engineering Division of Eastman Kodak Company in Rochester, NY. From 1992 to 2004 he worked in Turkey specializing in education and cultural exchange. His current research interests are in the area of fMRI and mood disorders.